

# Femtosecond Excited-State Dynamics of an Iron(II) Polypyridyl Solar Cell Sensitizer Model

Jeremy E. Monat and James K. McCusker\*

Contribution from the Department of Chemistry, University of California at Berkeley, Berkeley, California 94720-1460

Received July 12, 1999. Revised Manuscript Received January 18, 2000

**Abstract:** Time-resolved electronic absorption spectroscopy on a  $\sim 100$  fs time scale has been used to study excited-state dynamics in an Fe<sup>II</sup> polypyridyl complex. [Fe(tren(py)<sub>3</sub>)]<sup>2+</sup>, where tren(py)<sub>3</sub> is tris(2-pyridylmethyliminoethyl)amine, forms a <sup>1</sup>MLCT excited state upon irradiation at 400 nm and is known from previous studies to undergo relaxation to a low-lying ligand-field state having  $S = 2$ . Static absorption measurements on the low-spin parent complex and a high-spin analogue have been used to identify spectroscopic signatures for the  $S = 0$  and  $S = 2$  ligand-field states, respectively. Comparison of these data with femtosecond and nanosecond differential absorption spectra establishes that the net  $\Delta S = 2$  intersystem crossing is essentially complete in well under 1 ps. Spectroelectrochemistry on [Fe(tren(py)<sub>3</sub>)]<sup>2+</sup> has also been used to find an absorption feature characteristic of the initially formed <sup>1</sup>MLCT state at  $\lambda \gtrsim 600$  nm. Analysis of single-wavelength kinetics data in this spectral region reveals that the charge-transfer  $\rightarrow$  ligand-field manifold conversion, observed here for the first time, occurs with a nearly instrument-response limited time constant of less than 100 fs. Additional dynamics occurring with a time constant of  $8 \pm 3$  ps are tentatively assigned as vibrational cooling in the high-spin ligand-field state. The ultrafast intersystem crossing is interpreted as calling into question the utility of spin selection rules for understanding and predicting excited-state relaxation dynamics in transition metal complexes, whereas the sub-100 fs MLCT  $\rightarrow$  LF conversion is discussed in terms of its implications for the dynamics of electron injection in Fe<sup>II</sup>-sensitized TiO<sub>2</sub>-based solar cells.

## Introduction

Intersystem crossing is of central importance in the excited-state dynamics of most photochemical and photophysical processes involving transition metals.<sup>1–7</sup> For example, intersystem crossing removes spin-allowed relaxation pathways to the ground state, often yielding a longer-lived excited state and thus increased intermolecular reactivity. The early development of models for excited state relaxation dynamics in metal complexes was largely based on guidelines derived from the more mature field of organic photochemistry.<sup>8–10</sup> Such models suggested an ordering of relative rates in which the molecule first vibrationally cools in its initially prepared excited state, relaxes to the lowest energy excited state having the same total spin (internal conversion, IC), and then perhaps undergoes

intersystem crossing (ISC) to a state of differing spin if one of lower energy exists; in principle, this last step will compete with ground-state recovery via IC.

The details of such excited-state dynamics in transition complexes are critically important in an application that has seen rapidly growing interest over the past decade, namely sensitization of wide band gap semiconductors to achieve solar energy conversion. The pioneering research of Grätzel and co-workers<sup>11–13</sup> utilized transition metal-based complexes to effect electron injection into TiO<sub>2</sub> from a metal-to-ligand charge-transfer (MLCT) excited state of the chromophore. Such devices with overall efficiencies exceeding 10% have been reported.<sup>11–13</sup> The most successful device thus far employs a Ru<sup>II</sup> polypyridyl complex as the sensitizer. The mechanistic question addressed in part by the experiments reported herein concerns whether electron injection is occurring from the initially formed excited state (e.g., the <sup>1</sup>MLCT of the Ru<sup>II</sup> system) or after relaxation to the lowest energy excited state of the chromophore (e.g., the <sup>3</sup>MLCT). This issue is not merely one of academic interest: if a molecule need only have an initial excited state capable of electron injection, the number of sensitizer candidates and energy conversion efficiency could in principle be greatly increased.<sup>14,15</sup> Conventional wisdom posited that electron transfer should occur from a long-lived excited state based largely on Kasha's rule and the expectation that thermalization within

(1) Roundhill, D. M. *Photochemistry and Photophysics of Metal Complexes*; Plenum Press: New York, 1994.

(2) Ferraudi, G. J. *Elements of Inorganic Photochemistry*; John Wiley and Sons: New York, 1988.

(3) Yersin, H.; Vogler, A., Eds. *Photochemistry and Photophysics of Coordination Compounds*; Springer-Verlag: Berlin, 1987.

(4) Geoffroy, G. L.; Wrighton, M. S. *Organometallic Photochemistry*; Academic Press: New York, 1979.

(5) Ramamurthy, V.; Schanze, K. S., Eds. *Organic and Inorganic Photochemistry*; M. Dekker: New York, 1998.

(6) Adamson, A. W.; Fleischauer, P. D., Eds. *Concepts of Inorganic Photochemistry*; Wiley: New York, 1975.

(7) Kettle, S. F. A. *Physical Inorganic Chemistry*; Spektrum: Oxford, 1996.

(8) Turro, N. J. *Modern Molecular Photochemistry*; University Science Books: Mill Valley, CA, 1991.

(9) Coxon, J. M.; Halton, B. *Organic Photochemistry*, 2nd ed.; Cambridge University Press: Cambridge, 1987.

(10) Cowan, D. O.; Drisko, R. L. *Elements of Organic Photochemistry*; Plenum Press: New York, 1976.

(11) O'Regan, B.; Grätzel, M. *Nature* **1991**, 353, 737.

(12) Nazeeruddin, M. K.; Kay, A.; Rodicio, I.; Humphrybaker, R.; Müller, E.; Liska, P.; Vlachopoulos, N.; Grätzel, M. *J. Am. Chem. Soc.* **1993**, 115, 6382.

(13) Kalyanasundaram, K.; Grätzel, M. *Coord. Chem. Rev.* **1998**, 177, 347.

(14) Ferrere, S.; Gregg, B. A. *J. Am. Chem. Soc.* **1998**, 120, 843.

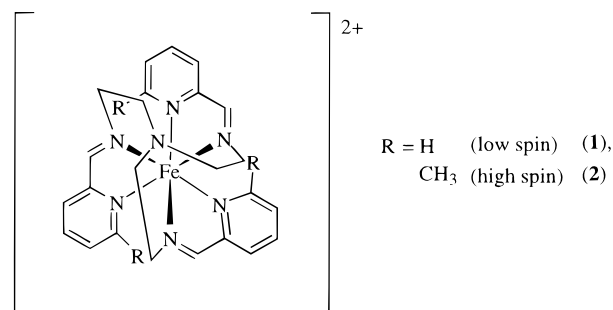
the excited electronic manifold of the chromophore will precede reactivity. Recently, this assumption has been called into question based on results from a number of groups. For example, following photoinduced intervalence charge transfer in mixed-valence dinuclear complexes, subpicosecond back-electron transfer from a nonthermalized excited state across a bridging group has been observed in  $[(\text{NH}_3)_5\text{Ru}^{\text{III}}\text{NCRu}^{\text{II}}(\text{CN})_5]^-$  and  $[(\text{NH}_3)_5\text{Ru}^{\text{III}}\text{NCFe}^{\text{II}}(\text{CN})_5]^-$  by Barbara and Hupp,<sup>16–18</sup> as well as by Woodruff and co-workers in  $[(\text{NH}_3)_5\text{Ru}^{\text{III}}\text{NCRu}^{\text{II}}(\text{CN})_5]^-$  and  $[(\text{NH}_3)_5\text{Os}^{\text{III}}\text{NCOs}^{\text{II}}(\text{CN})_5]^-$ .<sup>19,20</sup> In addition, reactivity from the Franck–Condon region was very recently demonstrated by Farrell et al., who noted that the branching ratio between CO loss and nonradiative relaxation is highly dependent on the excitation wavelength following <sup>1</sup>MLCT excitation of  $\text{Cr}(\text{CO})_4(\text{bpy})$ .<sup>21</sup> Similarly, work in our group on the excited-state dynamics of simple tris-bipyridyl ruthenium(II) complexes suggests vibrational cooling to be the slowest process prior to ground-state recovery, with <sup>1</sup>MLCT  $\rightarrow$  <sup>3</sup>MLCT intersystem crossing appearing to occur an order of magnitude or more faster.<sup>22</sup> Transfer of nonthermalized charge carriers (holes) across the  $\text{TiO}_2(001)/\text{KSCN}(\text{aq})$  interface has also been recently noted.<sup>23</sup>

With specific regard to titanium dioxide solar cells, several groups have studied electron injection in  $\text{Ru}^{\text{II}}$ -sensitized  $\text{TiO}_2$  to elucidate the mechanism of this important first step for photovoltaic conversion.<sup>13,24–29</sup> Perhaps the most compelling data are those of Lian and co-workers, who observed a charge injection time of less than 50 fs by direct detection of electrons in the semiconductor following charge-transfer excitation of the sensitizer  $\text{Ru}(\text{dcbpy})_2(\text{NCS})_2$  (commonly known as N3), where dcbpy is 4,4'-dicarboxy-2,2'-bipyridine;<sup>28</sup> similar subpicosecond injection was observed using coumarin 343 and  $[\text{Fe}(\text{CN})_6]^{4-}$ .<sup>30,31</sup> Moser and Grätzel recently used variable excitation wavelength studies to suggest that electron injection into semiconductors can occur from nonthermalized vibrational levels of a dye.<sup>27,32</sup>

Unfortunately, the question of whether electron injection occurs from an upper *electronic* excited state (e.g., the initially prepared <sup>1</sup>MLCT) is difficult to answer for a  $\text{Ru}^{\text{II}}$  polypyridyl

photosensitizer as both the initial and long-lived excited states may have sufficient energy and redox-active orbital overlap with the  $\text{TiO}_2$  conduction band to yield charge injection. Such is not the case for  $\text{Fe}^{\text{II}}$  polypyridyl complexes: despite having the same <sup>1</sup>A<sub>1</sub> ground state, the lowest energy excited state of these compounds (and likely  $[\text{Fe}^{\text{II}}(\text{CN})_6]^{4-}$ , as well) is a ligand-field state due to the reduction in d-orbital splitting of first- versus second-row transition metals. This type of state is not expected to inject efficiently because the excited configuration is localized on the metal center, spatially distant from the titanium dioxide nanoparticles; in addition, the driving force for electron injection from this state will likely be considerably less than that for the <sup>1</sup>MLCT state.<sup>14</sup> However, Ferrere and Gregg have recently demonstrated photoelectrochemical conversion in a titanium dioxide-based solar cell employing an  $\text{Fe}^{\text{II}}$  polypyridyl sensitizer,  $\text{Fe}(\text{dcbpy})_2(\text{CN})_2$ . To the extent that the above arguments apply to this compound when bound to the surface of  $\text{TiO}_2$ , their observations imply electron injection from the initially formed MLCT excited state of this system. In terms of chromophore design for  $\text{TiO}_2$ -based photovoltaics, this result is potentially very noteworthy.

To ascertain what is implied by the observations of Ferrere and Gregg, a more detailed understanding of the ultrafast dynamics of  $\text{Fe}^{\text{II}}$  polypyridyls is necessary; we have therefore undertaken such a study. In this article, we report data from femtosecond time-resolved absorption measurements on  $[\text{Fe}(\text{tren}(\text{py})_3)]^{2+}$  (**1**), where  $\text{tren}(\text{py})_3$  is tris(2-pyridylmethyliminoethyl)amine. This compound is a member of a series of



molecules that have been examined extensively for their spin-crossover behavior and as such provides a well-understood template for investigating excited-state dynamics in  $\text{Fe}^{\text{II}}$  systems.<sup>33–48</sup> It has been shown previously by a number of workers<sup>33–37</sup> that <sup>1</sup>A<sub>1</sub>  $\rightarrow$  <sup>1</sup>MLCT excitation of such compounds results in the formation of the high-spin ligand-field state (<sup>5</sup>T<sub>2</sub>) as the lowest energy excited state. The ultrafast spectroscopy of these types of systems also has been investigated;<sup>47,48</sup> however, these studies, while clearly suggestive of a subpicosecond <sup>1</sup>MLCT  $\rightarrow$  <sup>5</sup>T<sub>2</sub> conversion, revealed only an instrument-limited ground-state bleach as the signature for <sup>5</sup>T<sub>2</sub> formation. The data presented herein definitively establish the ultrafast nature of this formally  $\Delta S = 2$  transition. In addition, we report the first observation of evolution from the initially formed <sup>1</sup>MLCT excited state. The results clearly demonstrate that charge-transfer to ligand-field manifold conversion occurs at a rate exceeding  $10^{13} \text{ s}^{-1}$ , suggesting that hot electron injection is a likely, if not necessary, mechanism for sensitization of  $\text{TiO}_2$  by  $\text{Fe}^{\text{II}}$ -based chromophores.

- (15) Damrauer, N. H.; Cerullo, G.; Yeh, A.; Boussie, T. R.; Shank, C. V.; McCusker, J. K. *Science* **1997**, *275*, 54.  
 (16) Reid, P. J.; Silva, C.; Barbara, P. F.; Karki, L.; Hupp, J. T. *J. Phys. Chem.* **1995**, *99*, 2609.  
 (17) Tominaga, K.; Kliner, D. A. V.; Johnson, A. E.; Levinger, N. E.; Barbara, P. F. *J. Chem. Phys.* **1993**, *98*, 1228.  
 (18) Walker, G. C.; Barbara, P. F.; Doorn, S. K.; Dong, Y. H.; Hupp, J. T. *J. Phys. Chem.* **1991**, *95*, 5712.  
 (19) Doorn, S. K.; Dyer, R. B.; Stoutland, P. O.; Woodruff, W. H. *J. Am. Chem. Soc.* **1993**, *115*, 6398.  
 (20) Doorn, S. K.; Stoutland, P. O.; Dyer, R. B.; Woodruff, W. H. *J. Am. Chem. Soc.* **1992**, *114*, 3133.  
 (21) Farrell, I. R.; Matousek, P.; Vlček, A. *J. Am. Chem. Soc.* **1999**, *121*, 5296.  
 (22) Damrauer, N. H.; McCusker, J. K. *J. Phys. Chem. A* **1999**, *103*, 8440.  
 (23) Morishita, T.; Hibara, A.; Sawada, T.; Tsuyumoto, I. *J. Phys. Chem. B* **1999**, *103*, 5984.  
 (24) Heimer, T. A.; Heilweil, E. J. *J. Phys. Chem. B* **1997**, *101*, 10990.  
 (25) Tachibana, Y.; Moser, J. E.; Grätzel, M.; Klug, D. R.; Durrant, J. R. *J. Phys. Chem.* **1996**, *100*, 20056.  
 (26) Moser, J. E.; Bonnôte, P.; Grätzel, M. *Coord. Chem. Rev.* **1998**, *171*, 245.  
 (27) Moser, J. E.; Grätzel, M. *Chimia* **1998**, *52*, 160.  
 (28) Ellingson, R. J.; Asbury, J. B.; Ferrere, S.; Ghosh, H. N.; Sprague, J. R.; Lian, T. Q.; Nozik, A. J. *J. Phys. Chem. B* **1998**, *102*, 6455.  
 (29) Hannappel, T.; Burfeindt, B.; Storck, W.; Willig, F. *J. Phys. Chem. B* **1997**, *101*, 6799.  
 (30) Ghosh, H. N.; Asbury, J. B.; Lian, T. Q. *J. Phys. Chem. B* **1998**, *102*, 6482.  
 (31) Ghosh, H. N.; Asbury, J. B.; Weng, Y. X.; Lian, T. Q. *J. Phys. Chem. B* **1998**, *102*, 10208.  
 (32) We note that Thompson et al. demonstrated that electron injection can occur on the nanosecond time scale from a long-lived state afforded by reductive quenching of an excited sensitizer: Thompson, D. W.; Kelly, C. A.; Farzad, F.; Meyer, G. J. *Langmuir* **1999**, *15*, 650.

## Experimental Section

**Materials.**  $[\text{Fe}(\text{tren}(\text{py})_3)]^{2+}$  and  $[\text{Fe}(\text{tren}(6\text{-Me-py})_3)]^{2+}$  were each prepared as the  $\text{PF}_6^-$  salt according to literature methods.<sup>38</sup> The compounds analyzed satisfactorily by electrospray mass spectrometry and elemental analysis performed by the Analytical Facilities of the University of California at Berkeley. Spectroscopic studies were carried out in acetonitrile purchased from Fisher. HPLC grade solvent was used as received while Certified A.C.S. grade was distilled over  $\text{CaH}_2$  prior to use.

**Cyclic Voltammetry.** Cyclic voltammograms were collected under an inert atmosphere using a BAS 50 W Voltammetric Analyzer at a scan rate of  $100 \text{ mV s}^{-1}$  with a standard three-electrode configuration consisting of a Pt working electrode, a Pt wire counter electrode, and a  $\text{Ag}/\text{AgNO}_3$  reference electrode. The  $\text{CH}_3\text{CN}$  solution contained  $\sim 0.1 \text{ M}$  tetrabutylammonium hexafluorophosphate as supporting electrolyte.

**Spectroelectrochemistry.** Spectroelectrochemical data were acquired as reported elsewhere.<sup>22</sup> Oxidative (and reductive) bulk electrolyses were found to be irreversible when carried out over an extended period of time. The spectra reported therefore correspond to electrolysis times for which the isosbestic point between the parent and oxidized (reduced) complex was still present.

**Nanosecond Time-Resolved Spectroscopy.** The nanosecond difference spectrum was acquired using a Nd:YAG-based transient absorption spectrometer that is described elsewhere.<sup>49</sup> The spectrum was generated by plotting the amplitude from single-exponential fits to the excited-state decay kinetics at each probe wavelength.

**Femtosecond Transient Absorption Data.** Ultrafast transient absorption data were acquired using a Ti:sapphire-based regeneratively amplified femtosecond absorption spectrometer. Details regarding this apparatus can be found elsewhere.<sup>22</sup> Pump energies used in these experiments were typically  $6.5 \mu\text{J}/\text{pulse}$  for single wavelength traces and  $11 \mu\text{J}/\text{pulse}$  for full spectra; signal linearity with respect to pump energy was verified from ca. 5 to  $11 \mu\text{J}/\text{pulse}$ . The sample solution was placed in a 1 mm path length cell with optical densities at the pump wavelength (400 nm) of  $\sim 0.95$  for single wavelength data collection and  $\sim 0.2$  for acquisition of spectra. No sample concentration dependence was observed in the data. Samples were flowed for full spectra data; however, no sample degradation was evident for either data set based on comparisons of ground-state electronic absorption spectra before and after pump-probe experiments.

A weak signal from the pure solvent around  $\Delta t = 0$  ( $< 6\%$  of the peak signal amplitude for the sample near  $\Delta t = 0$ ) was subtracted from the single-wavelength data. These data were then fit via iterative reconvolution (using a Gaussian instrument response function) to a biexponential function with an offset, denoting two relaxation processes

(33) Xie, C.-L.; Hendrickson, D. N. *J. Am. Chem. Soc.* **1987**, *109*, 6981.

(34) Beattie, J. K. *Adv. Inorg. Chem.* **1988**, *32*, 1.

(35) Hauser, A. *Commun. Inorg. Chem.* **1995**, *17*, 17 and references therein.

(36) Gütllich, P. *Mol. Cryst. Liq. A* **1997**, *305*, 17 and references therein.

(37) McCusker, J. K.; Rheingold, A. L.; Hendrickson, D. N. *Inorg. Chem.* **1996**, *35*, 2100 and references therein.

(38) Conti, A. J.; Xie, C.-L.; Hendrickson, D. N. *J. Am. Chem. Soc.* **1989**, *111*, 1171.

(39) Hoselton, M. A.; Wilson, L. J.; Drago, R. S. *J. Am. Chem. Soc.* **1975**, *97*, 1722.

(40) König, E. *Struct. Bond.* **1991**, *76*, 51.

(41) Hauser, A. *Coord. Chem. Rev.* **1991**, *111*, 275.

(42) Gütllich, P.; Jung, J. *J. Mol. Struct.* **1995**, *347*, 21.

(43) Gütllich, P.; Hauser, A. *Coord. Chem. Rev.* **1990**, *97*, 1.

(44) Wu, C. C.; Jung, J.; Gantzel, P. K.; Gütllich, P.; Hendrickson, D. N. *Inorg. Chem.* **1997**, *36*, 5339 and references therein.

(45) Schenker, S.; Hauser, A.; Dyson, R. M. *Inorg. Chem.* **1996**, *35*, 4676 and references therein.

(46) Al-Obaidi, A. H. R.; Jensen, K. B.; McGarvey, J. J.; Toftlund, H.; Jensen, B.; Bell, S. E. J.; Carroll, J. G. *Inorg. Chem.* **1996**, *35*, 5055 and references therein.

(47) McCusker, J. K.; Walda, K. N.; Dunn, R. C.; Simon, J. D.; Magde, D.; Hendrickson, D. N. *J. Am. Chem. Soc.* **1992**, *114*, 6919.

(48) McCusker, J. K.; Walda, K. N.; Dunn, R. C.; Simon, J. D.; Magde, D.; Hendrickson, D. N. *J. Am. Chem. Soc.* **1993**, *115*, 298.

(49) Damrauer, N. H.; Boussie, T. R.; Devenney, M.; McCusker, J. K. *J. Am. Chem. Soc.* **1997**, *119*, 8253.

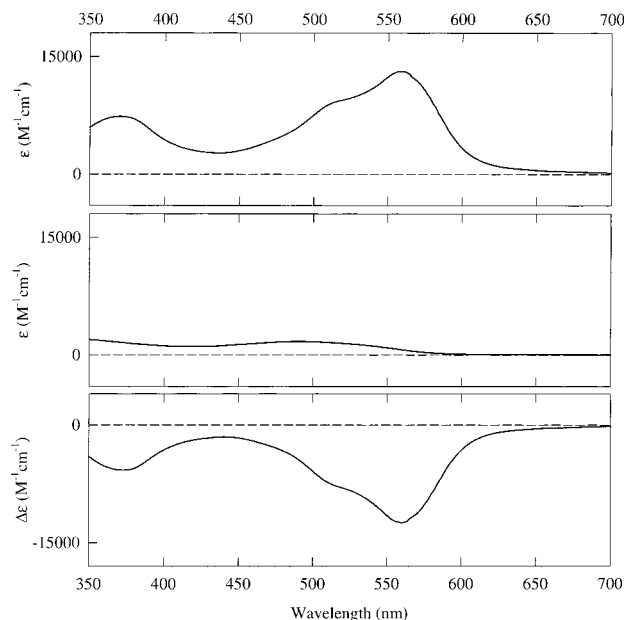


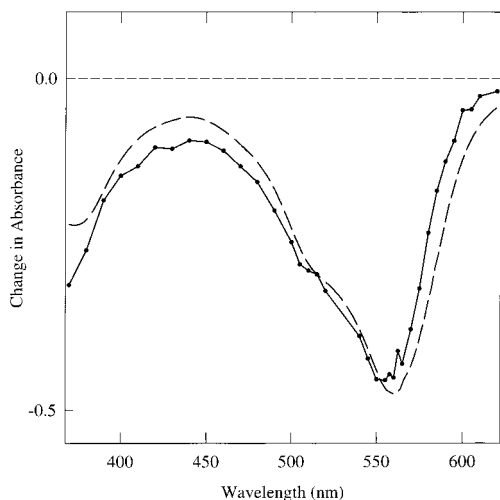
**Figure 1.** (Top) Ground-state absorption spectrum of  $[\text{Fe}(\text{tren}(\text{py})_3)](\text{PF}_6)_2$  (**1**) in  $\text{CH}_3\text{CN}$ . (Middle) Ground-state absorption spectrum of  $[\text{Fe}(\text{tren}(6\text{-Me-py})_3)](\text{PF}_6)_2$  (**2**) in  $\text{CH}_3\text{CN}$ . (Bottom) Molar absorptivity difference spectrum,  $\Delta\epsilon$ , between  $[\text{Fe}(\text{tren}(\text{py})_3)]^{2+}$  and  $[\text{Fe}(\text{tren}(6\text{-Me-py})_3)]^{2+}$ .

occurring on a subnanosecond time scale; the offset corresponds to the transient differential absorption of the  $^5\text{T}_2$  state observed previously. The initial position of  $\Delta t = 0$  for single wavelength kinetics traces was determined from a cross-correlation of the 400 nm pump pulse with the appropriate probe wavelength via two-photon absorption in  $\alpha,\alpha,\alpha$ -trichlorotoluene. It was consistently found to be necessary to shift the zero-of-time by 30 or 40 fs to obtain a reasonable fit; this shifted zero-of-time is used as  $\Delta t = 0$  in Figure 7. Within an approximately 30 fs window for  $\Delta t = 0$ , the fit converged well and the optimized time constants were found to be independent of the zero-of-time placement within the estimated experimental error. The full-width at half-maximum (fwhm) of the Gaussian instrument response function was that experimentally measured from the cross-correlation. This fwhm was typically held constant until a reasonable fit was obtained, then allowed to vary to obtain the final parameters. Reported time constants reflect five independent data sets individually fit using this procedure.

## Results and Discussion

### Formation of the Long-Lived Ligand-Field Excited State.

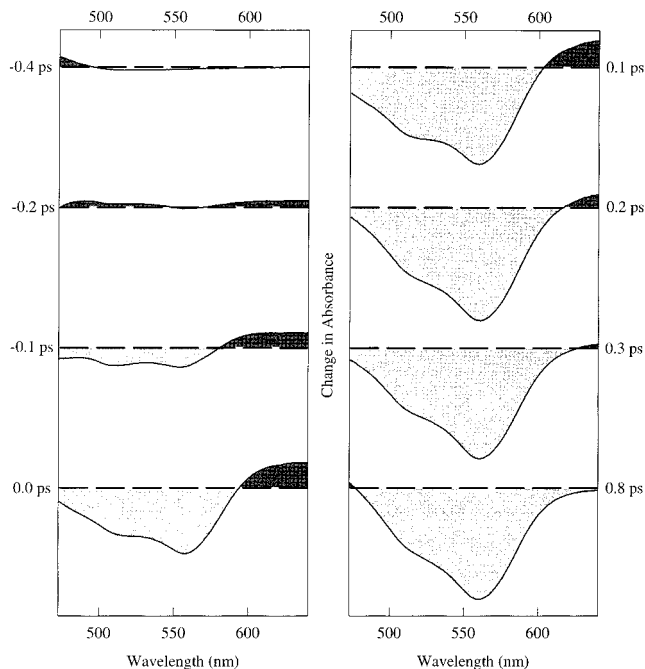
One of the goals of this work was to establish the time scale for converting from a charge-transfer to a ligand-field manifold. To do this, it is important to identify spectroscopic features of both manifolds such that they can be distinguished from each other in a time-resolved optical experiment. The compound we have chosen is ideally suited for this purpose due to its near-spin-crossover character. Thus, we can estimate the excited-state difference spectrum of the  $^5\text{T}_2$  ligand-field state of  $[\text{Fe}(\text{tren}(\text{py})_3)]^{2+}$  by taking advantage of the fact that substitution of  $\text{CH}_3$  groups in the 6-position of the pyridyl rings (yielding  $[\text{Fe}(\text{tren}(6\text{-Me-py})_3)]^{2+}$ , **2**) results in the stabilization of the  $^5\text{T}_2$  state as the ground state at room temperature.<sup>38,39</sup> To a good approximation, the molar absorptivity difference ( $\Delta\epsilon$ ) spectrum between the methylated and unmethylated compounds should therefore correspond to the time-resolved difference spectrum expected once the  $^5\text{T}_2$  excited state of  $[\text{Fe}(\text{tren}(\text{py})_3)]^{2+}$  is formed. Absorption spectra for both compounds as well as their difference are presented in Figure 1. As expected for a metal-to-ligand charge-transfer band, the intensity of the MLCT



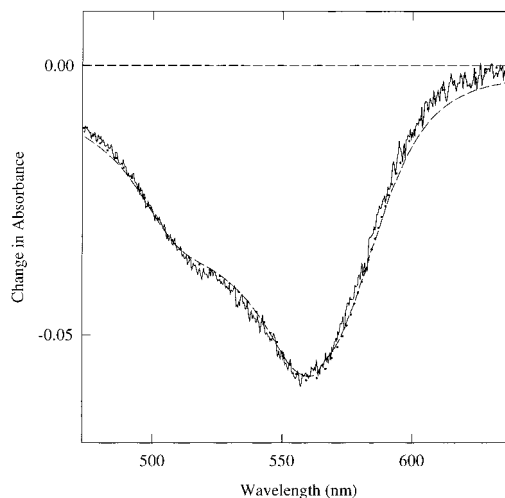
**Figure 2.** Nanosecond time-resolved absorption difference spectrum for  $[\text{Fe}(\text{tren}(\text{py})_3)](\text{PF}_6)_2$  in  $\text{CH}_3\text{CN}$  following  $\sim 10$  ns, 3 mJ excitation at 532 nm (points and solid line). The dashed line is the arbitrarily scaled differential absorption spectrum generated from high-spin  $[\text{Fe}(\text{tren}(6\text{-Me-py})_3)]^{2+}$  and low-spin  $[\text{Fe}(\text{tren}(\text{py})_3)]^{2+}$  (Figure 1, bottom panel).

band(s) of the high-spin molecule is attenuated relative to the low-spin species due to elongation of the Fe–N bond in the high-spin state.<sup>39</sup> On the basis of these spectra, we can expect to observe a transient bleach at all wavelengths in this region of the spectrum upon formation of the  $^5\text{T}_2$  excited state in  $[\text{Fe}(\text{tren}(\text{py})_3)]^{2+}$ . The assignment of the high-spin ligand-field state as the long-lived excited state<sup>38</sup> is supported by comparing the nanosecond difference spectrum with the calculated  $\Delta\epsilon$  spectrum from Figure 1; this comparison is shown in Figure 2. The spectra are clearly in good agreement, thereby confirming that the  $^5\text{T}_2$  state is the last excited state accessed by  $[\text{Fe}(\text{tren}(\text{py})_3)]^{2+}$  following  $^1\text{MLCT}$  excitation.

The time scale for forming this long-lived excited state may thus be estimated by comparing both the nanosecond and molar absorptivity difference spectra with femtosecond transient absorption spectra.<sup>15</sup> In Figure 3 we present femtosecond differential absorption spectra at various time delays following  $\sim 130$  fs excitation of  $[\text{Fe}(\text{tren}(\text{py})_3)](\text{PF}_6)_2$  in  $\text{CH}_3\text{CN}$  at 400 nm. The spectra are distorted somewhat at early times due to a ca. 250 fs chirp in the continuum probe across the spectral window; redder wavelengths therefore appear to evolve at later times relative to the bluer wavelengths. However, noting especially the conversion of the short-lived absorptive feature near 620 nm to a weak bleach (see below), it is clear that the basic spectroscopic features of the  $^5\text{T}_2$  state are established very early in the relaxation process. A comparison of femtosecond difference spectra acquired at  $\Delta t = 0.5$  and 6.3 ps shows remarkable agreement with each other and the anticipated  $\Delta A$  spectrum for the high-spin/low-spin conversion, Figure 4, establishing that the  $^5\text{T}_2$  state is formed in well under 1 ps. The  $\Delta A$  spectrum was calculated from the  $\Delta\epsilon$  spectrum according to the equation  $\Delta A = \Delta\epsilon \cdot l \cdot [\text{Fe}] \cdot x$ , where  $l$  is the path length in cm,  $[\text{Fe}]$  represents the nominal concentration of  $[\text{Fe}(\text{tren}(\text{py})_3)]^{2+}$ , and  $x$  is a scaling factor between 0 and 1. The parameter  $x$  reflects the fraction of excited state (i.e.,  $^5\text{T}_2$ ) that is produced and then probed in the femtosecond measurement according to the expression  $[\text{Fe}(\text{tren}(\text{py})_3)]^{2+} = x[\text{Fe}]$  ( $x$  should not, therefore, be confused with a quantum yield for  $^5\text{T}_2$  formation).<sup>50</sup> It was chosen to achieve the best match with the femtosecond difference spectrum, namely 0.101, to give the dashed line in



**Figure 3.** Femtosecond differential absorption spectra for  $[\text{Fe}(\text{tren}(\text{py})_3)](\text{PF}_6)_2$  in  $\text{CH}_3\text{CN}$  following  $\sim 130$  fs excitation at 400 nm. The labels indicate delay times relative to  $\Delta t = 0$  as determined by cross-correlation between the 400 nm pump and  $\lambda_{\text{probe}} = 620$  nm. The apparent spectral shift from short to long wavelengths is largely due to temporal chirp in the continuum probe ( $\sim 250$  fs for the entire spectral window shown).



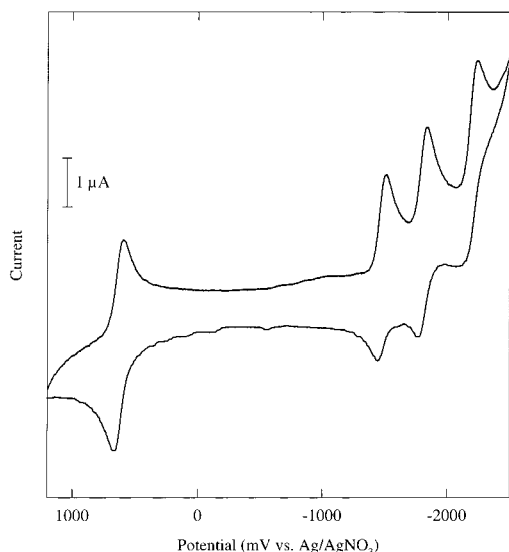
**Figure 4.** An overlay of femtosecond difference spectra at  $\Delta t = 0.5$  ps (dotted line) and 6.3 ps (solid line) with a scaled  $\Delta A$  spectrum generated from the high-spin  $[\text{Fe}(\text{tren}(6\text{-Me-py})_3)]^{2+}$ /low-spin  $[\text{Fe}(\text{tren}(\text{py})_3)]^{2+}$   $\Delta\epsilon$  spectrum (dashed line). See text for further details.

Figure 4. This value is in accord with the ca. 10% excited state population typically achieved in transient absorption measurements.

**Evolution from the Initial Charge-Transfer State.** As we have recently learned in femtosecond studies of  $\text{Ru}^{\text{II}}$  polypyridyl complexes,<sup>15,22,51</sup> excited-state dynamics in metal complexes are

(50) The quantum yield of formation of the  $^5\text{T}_2$  state following  $^1\text{MLCT}$  excitation in related  $\text{Fe}^{\text{II}}$  complexes has been reported to be  $\sim 1$ . See: Creutz, C.; Chou, M.; Netzel, T. L.; Okumura, M.; Sutin, N. *J. Am. Chem. Soc.* **1980**, *102*, 1309. Bergkamp, M. A.; Chang, C.-K.; Netzel, T. L. *J. Phys. Chem.* **1983**, *87*, 4441.

(51) Damrauer, N. H.; Curtright, A. E.; McCusker, J. K. Manuscript in preparation.



**Figure 5.** Cyclic voltammogram of  $[\text{Fe}(\text{tren}(\text{py})_3)](\text{PF}_6)_2$  in  $\text{CH}_3\text{CN}$ .

best examined by probing in regions of excited-state absorptions<sup>22,51</sup> or bleach regions where significant evolution of the excited-state absorption profile is occurring.<sup>15</sup> Spectroelectrochemical data have proven to be extremely useful for gaining insight into the nature of absorptive features in the excited-state spectrum.<sup>22,51,52</sup> In the case of  $[\text{Fe}(\text{tren}(\text{py})_3)]^{2+}$ , charge-transfer excitation ultimately results in the formation of a ligand-field state that is expected to have a markedly different absorption spectrum than the Franck–Condon MLCT state. We can therefore use spectroelectrochemistry to sketch a picture of the Franck–Condon state and subsequently determine appropriate wavelengths for monitoring excited-state evolution from the charge-transfer to the ligand-field manifold. To determine appropriate potentials for bulk oxidation and reduction, cyclic voltammetry was performed on an acetonitrile solution of  $[\text{Fe}(\text{tren}(\text{py})_3)](\text{PF}_6)_2$ ; the resulting voltammogram is shown in Figure 5. As expected, it shows a single oxidative wave corresponding to  $\text{Fe}^{\text{II}} \rightarrow \text{Fe}^{\text{III}}$  oxidation and three reductive waves assigned to three successive reductions of the pyridyl moieties.

Oxidative and reductive spectroelectrochemical data for  $[\text{Fe}(\text{tren}(\text{py})_3)](\text{PF}_6)_2$  in  $\text{CH}_3\text{CN}$  were obtained following partial bulk electrolysis at potentials of +0.77 V and -1.58 V vs Ag/AgNO<sub>3</sub>, respectively; these spectra are shown in Figure 6 (middle and bottom panels, respectively). They reveal net absorptive losses in the region of the lowest-energy ground-state charge-transfer band (centered at 560 nm), as expected: both oxidation and reduction of  $[\text{Fe}(\text{tren}(\text{py})_3)]^{2+}$  will result in attenuation of MLCT intensity due to complete (oxidative:  $[\text{Fe}^{\text{II}}(\text{L})_3]^{2+} \rightarrow [\text{Fe}^{\text{III}}(\text{L})_3]^{3+}$ ) or partial (reductive:  $[\text{Fe}^{\text{II}}(\text{L})_3]^{2+} \rightarrow [\text{Fe}^{\text{II}}(\text{L})_2(\text{L}^-)]^{1+}$ ) loss of the requisite chromophore. Moreover, both the oxidative and reductive spectra show absorptions at longer wavelengths ( $\lambda \geq 600$  nm) these bands are assigned as LMCT (oxidative) and ligand  $\pi^* \rightarrow \pi^*$  (reductive) in nature. This long-wavelength region corresponds to a bleach in the high-spin/low-spin difference spectrum (Figure 1, bottom panel). We can therefore conclude that transient absorptions in this long-wavelength region will be diagnostic for a charge-transfer (i.e.,  $[\text{Fe}^{\text{III}}(\text{L})_2(\text{L}^-)]^{2+}$ ) chromophore, and the associated decay kinetics an indication of the time scale with which the system evolves away from the initially formed <sup>1</sup>MLCT state back to the ligand-field manifold.

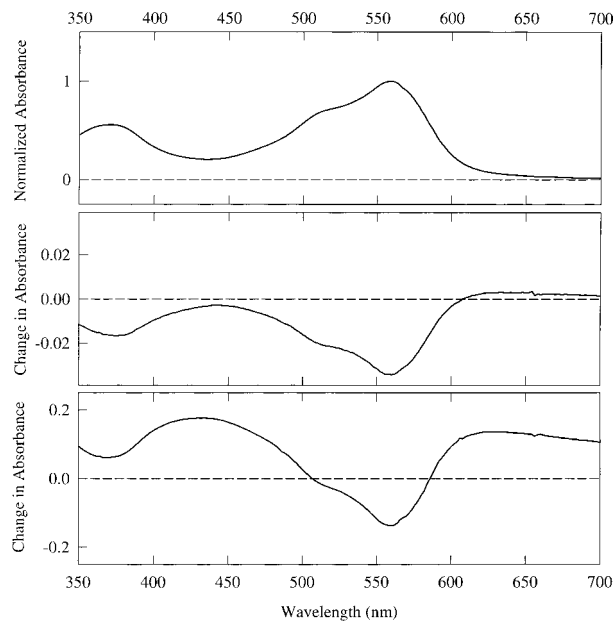


**Figure 6.** (Top) Ground-state absorption spectrum for  $[\text{Fe}(\text{tren}(\text{py})_3)](\text{PF}_6)_2$  in  $\text{CH}_3\text{CN}$ . (Middle) Oxidative difference spectrum for  $[\text{Fe}(\text{tren}(\text{py})_3)](\text{PF}_6)_2$  in  $\text{CH}_3\text{CN}$  after 3 min at a potential of +0.77 V vs Ag/AgNO<sub>3</sub>. (Bottom) Reductive difference spectrum for  $[\text{Fe}(\text{tren}(\text{py})_3)](\text{PF}_6)_2$  in  $\text{CH}_3\text{CN}$  after 6 min at a potential of -1.58 V vs Ag/AgNO<sub>3</sub>.

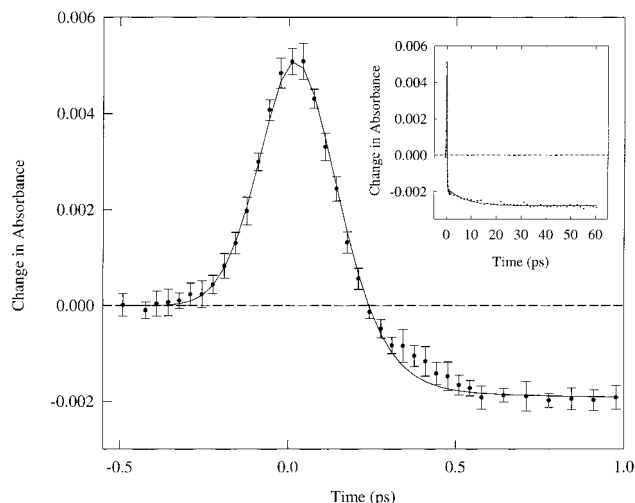


**Figure 7.** Single-wavelength kinetics trace for  $[\text{Fe}(\text{tren}(\text{py})_3)](\text{PF}_6)_2$  in  $\text{CH}_3\text{CN}$  at  $\lambda_{\text{probe}} = 620$  nm following  $\sim 130$  fs excitation at 400 nm. The inset shows data collected out to longer time delays. The line is the best-fit convolved biexponential having  $\tau_1 = 80 \pm 20$  fs and  $\tau_2 = 8 \pm 3$  ps.

Single wavelength femtosecond time-resolved absorption data were collected at a number of probe wavelengths following  $\sim 130$  fs excitation of  $[\text{Fe}(\text{tren}(\text{py})_3)](\text{PF}_6)_2$  in  $\text{CH}_3\text{CN}$  solution at 400 nm. For  $\lambda < 600$  nm, bleach features were observed to grow in essentially concomitant with excitation. This is similar to what had been observed previously for related systems,<sup>47,48</sup> but unfortunately is not discriminating for the charge-transfer state since a ground-state absorptive loss will in principle always accompany initial excitation. However, dramatically different results are obtained for  $\lambda_{\text{probe}} > 600$  nm: data collected at  $\lambda_{\text{probe}} = 620$  nm are illustrated in Figure 7. The signal consists of a nearly instrument response-limited absorption feature that decays to a bleach on the time scale of our experimental resolution. The instantaneous formation of the transient absorption and its immediate decay to a bleach indicate that the <sup>1</sup>MLCT state of

$[\text{Fe}(\text{tren}(\text{py})_3)]^{2+}$  relaxes extremely rapidly back to the ligand-field manifold.

The subpicosecond decay component, assigned to the charge-transfer to ligand-field manifold relaxation, was found to be nearly instrument-response limited: a best-fit value of  $\tau_1 = 80 \pm 20$  fs is shown for the data in Figure 7. These results are reminiscent of our previous report on rapid initial charge-transfer state relaxation in  $[\text{Ru}(\text{bpy})_3]^{2+}$ ,<sup>15</sup> as well as the rapid dynamics observed by Barbara and Hupp,<sup>16–18</sup> who demonstrated a ca. 80 fs back-electron-transfer rate in the mixed-valence complex  $[(\text{NH}_3)_5\text{Ru}^{\text{III}}\text{NCFe}^{\text{II}}(\text{CN})_5]^-$  following photoinduced intervalence charge transfer. Whether the subpicosecond process evident from Figure 7 corresponds to a direct  ${}^1\text{MLCT} \rightarrow {}^5\text{T}_2$  conversion is difficult to state unequivocally. However, analysis of these data does not suggest that any intermediate state is sampled between the  ${}^1\text{MLCT}$  and  ${}^5\text{T}_2$  states.

The subtle evolution noted at longer delay times occurs with a time constant of  $\tau_2 = 8 \pm 3$  ps. This feature is similar in nature to that observed following excitation of simple  $\text{Ru}^{\text{II}}$  polypyridyls such as  $[\text{Ru}(\text{dmb})_3]^{2+}$ .<sup>22,51</sup> Since the differential absorption features are essentially unaffected by these dynamics, we tentatively attribute these kinetics in  $[\text{Fe}(\text{tren}(\text{py})_3)]^{2+}$  to vibrational cooling on the  ${}^5\text{T}_2$  surface. We note that, based on previous studies of the spin-crossover behavior of the  $[\text{Fe}(\text{tren}(\text{6-Me-py})_{3-x}(\text{py})_x)]^{2+}$  ( $x = 0-3$ ) series,<sup>38</sup> the  ${}^1\text{A}_1/{}^5\text{T}_2$  energy gap can be estimated to be ca.  $1000 \text{ cm}^{-1}$ . Thus, excitation at 400 nm in this system requires nonradiative dissipation of ca.  $24\,000 \text{ cm}^{-1}$  of energy into the various degrees of freedom of the complex and/or the solvent bath. The rapid rate at which this apparently occurs as compared to simple metal carbonyls, for example,<sup>53–55</sup> is likely due to the large density of states (e.g., lower-frequency acceptor modes) associated with this molecule. Variable excitation wavelength studies or an infrared probe could more directly address the nature of this kinetic component.

### Concluding Comments

We have used a combination of static, nanosecond, and femtosecond spectroscopies to investigate excited-state dynamics in an  $\text{Fe}^{\text{II}}$  polypyridyl complex. Spectroelectrochemistry and a molar absorptivity difference spectrum between two closely related compounds helped to identify spectroscopic signatures for the initial and long-lived excited states, respectively, of  $[\text{Fe}(\text{tren}(\text{py})_3)]^{2+}$  following  ${}^1\text{A}_1 \rightarrow {}^1\text{MLCT}$  excitation in acetonitrile solution. Femtosecond and nanosecond difference spectra demonstrated that the long-lived  ${}^5\text{T}_2$  ligand-field state is formed in less than 1 ps. A convolved biexponential fit of kinetics data at 620 nm after  $\sim 130$  fs excitation at 400 nm further showed that the charge-transfer character of the excited state disappears with a time constant of less than 100 fs, indicating extremely rapid conversion from the charge-transfer to the ligand-field manifold. A second kinetic component with a time constant of  $8 \pm 3$  ps is tentatively assigned to vibrational relaxation in the  ${}^5\text{T}_2$  ligand-field state, the lowest energy excited state of the compound.

We believe that both the sub-100 fs loss of charge-transfer character and subpicosecond formation time of the  ${}^5\text{T}_2$  state in

this compound have important implications regarding the assignment of mechanisms for excited-state evolution in transition metal-based complexes. For example, the ultrafast conversion from the charge-transfer to the ligand-field manifold would appear to preclude complete thermalization in the  ${}^1\text{MLCT}$  state prior to surface crossing. In addition, the fact that a net  $\Delta S = 2$  conversion occurs on such a rapid time scale indicates the assumption that intersystem crossing will always be a relatively slow process is not correct, at least in the initial stages of excited-state relaxation. This does not imply that intersystem crossing *must* be fast, but in our opinion the identification of a particular step in a proposed relaxation sequence as “spin-forbidden” cannot be used as justification for ascribing a relative rate to that step. While the guidelines described in the introductory statements may have wider applicability in organic photophysics, we are finding with the present system and others<sup>15,22,51</sup> that the same rules are not useful for understanding and predicting the initial excited-state relaxation processes in transition metal complexes. The underlying reasons for this no doubt include the substantially larger spin-orbit coupling associated with transition metals, the larger number of electronic states present, and the larger Franck-Condon factors for higher vibrational quanta that are expected given the excited-state geometric distortions characteristic of charge-transfer and/or ligand-field excited states. All of these factors will contribute to extensive mixing among the various energy levels available to the system, both initially and as it evolves in time. We are continuing to examine these various issues in several different transition metal-based systems, both experimentally and theoretically, and will be reporting on some of these results soon.

Concerning the role of iron(II) polypyridyl complexes as titanium dioxide-based solar cell sensitizers, our results suggest that the charge injection likely occurs on the ultrafast time scale. That is, if the electronic structure and excited-state dynamics of the dye demonstrated by Ferrere and Gregg<sup>14</sup> anchored to  $\text{TiO}_2$  are similar to that of  $[\text{Fe}(\text{tren}(\text{py})_3)]^{2+}$  in acetonitrile solution, then electron injection would have to occur within about 100 fs to compete with intramolecular relaxation. This conjecture is consistent with the charge injection time of less than 50 fs observed by Ghosh et al. by direct detection of electrons in  $\text{TiO}_2$  sensitized by low-spin  $[\text{Fe}^{\text{II}}(\text{CN})_6]^{4-}$ .<sup>31</sup> Such rapid electron transfer raises the possibility that the initial electronic excited state, not just the long-lived one, is capable of charge injection. This allows one to consider molecules for use as surface-bound sensitizers which would not be useful photoelectrochemical agents in solution. One is left with the question of why charge injection is so rapid. It has been suggested that the continuum of states in the conduction band of titanium dioxide provides strong electronic coupling to the sensitizer excited state,<sup>12,25,56</sup> but the hypothesis that an accepting *band* is necessary for efficient injection is still being investigated.<sup>57</sup>

**Acknowledgment.** The authors are indebted to the Energy Sciences and Technology Program of the University of California Energy Institute and the Alfred P. Sloan Foundation (J.K.M.) for financial support. We also thank Dr. Niels Damrauer for several helpful discussions.

JA992436O

(53) King, J. C.; Zhang, J. Z.; Schwartz, B. J.; Harris, C. B. *J. Chem. Phys.* **1993**, *99*, 7595 and references therein.

(54) Harris, A. L.; Brown, J. K.; Harris, C. B. *Annu. Rev. Phys. Chem.* **1988**, *39*, 341.

(55) Arrivo, S. M.; Dougherty, T. P.; Grubbs, W. T.; Heilweil, E. J. *Chem. Phys. Lett.* **1995**, *235*, 247 and references therein.

(56) Rehm, J. M.; McLendon, G. L.; Nagasawa, Y.; Yoshihara, K.; Moser, J.; Grätzel, M. *J. Phys. Chem.* **1996**, *100*, 9577.

(57) Langdon, B. T.; MacKenzie, V. J.; Asunskis, D. J.; Kelley, D. F. *J. Phys. Chem. B* **1999**, *103*, 11176.